Beyond-mean-field results for atomic Bose-Einstein condensates at interaction strengths near Feshbach resonances: A many-body dimensional perturbation-theory calculation

B. A. McKinney, M. Dunn, and D. K. Watson*
Department of Physics and Astronomy, University of Oklahoma, Norman, Oklahoma 73019, USA
(Received 24 October 2003; published 13 May 2004)

We present semianalytical many-body results for energies and excitation frequencies for an inhomogeneous Bose-Einstein condensate over a wide range of atom numbers N for both small s-wave scattering lengths, typical of most laboratory experiments, and large scattering lengths, achieved by tuning through a Feshbach resonance. Our dimensional perturbation treatment includes two-body correlations at all orders and yields analytical results through first order by taking advantage of the high degree of symmetry of the condensate at the zeroth-order limit. Because N remains a parameter in our analytical results, the challenge of calculating energies and excitation frequencies does not rise with the number of condensate atoms. In this proof-of-concept paper the atoms are confined in a spherical trap and are treated as hard spheres. Our many-body calculations compare well to Gross-Pitaevskii results in the weakly interacting regime and depart from the mean-field approximation as the density approaches the strongly interacting regime. The excitation frequencies provide a particularly sensitive test of beyond-mean-field corrections. For example, for $N=2000$ atoms and an experimentally realized large scattering length of $a=0.433a_{ho}$ ($a_{ho}=\sqrt{\hbar/m\omega_{ho}}$) we predict a 75% shift from the mean-field breathing mode frequency.

DOI: 10.1103/PhysRevA.69.053611 PACS number(s): 03.75.−b

I. INTRODUCTION

The achievement of Bose-Einstein condensates (BEC) in magnetically trapped alkali-metal atoms has generated a considerable amount of experimental and theoretical activity in recent years. In typical BEC experiments, the average distance between the Bose atoms is much larger than the range of the atomic interactions, which is characterized by the s-wave scattering length a. The mean-field Gross-Pitaevskii (GP) equation has been instrumental in describing the properties of these weakly interacting condensates (see Ref. [1] for an extended review). A fundamental assumption underlying the derivation of the GP equation is that the precise interatomic potential can be replaced by the shape-independent approximation, also called the pseudopotential approximation, which uses a zero-range potential, as opposed to an extended potential with a well-defined shape:

$$V_{\text{pseudo}}(\mathbf{r}) = \frac{4\pi\hbar^2 a}{m}\delta(\mathbf{r}). \tag{1}$$

Despite its success in the weakly interacting regime, the GP equation does not include many-body effects, such as correlation, and its assumed shape-independent approximation breaks down in the strongly interacting regime [2]. Moreover, in recent experiments the presence of Feshbach resonances has enabled the creation of condensates in a regime in which the predictions of the mean-field theory are measurably lacking [3], allowing the condensate to act as a test bed for fundamental many-body physics beyond the mean-field approach. Recent theoretical studies, performed to quantify the breakdown of the mean-field theory and the shape-independent approximation, have been based on a number of theoretical methods including analytical corrections to the GP equation due to quantum fluctuations about the mean field [4,5] and a related approach from density-functional theory [6], while others are based on numerical calculations such as the diffusion Monte Carlo (DMC) method [7,8] or the correlated basis function approach [9,10]. In this paper, we further explore beyond-mean-field effects using many-body dimensional perturbation theory (DPT), a many-body approach that includes correlation beyond mean field at all perturbation orders. We use a shape-dependent interatomic potential, and the number of condensate atoms, N, appears as a parameter in our results which are analytical, thus making our many-body calculations for any N much less involved than even solving the mean-field GP equation. We also calculate excitation frequencies, which naturally arise out of our first-order, harmonic energy correction.

Even though this investigation of beyond-mean-field effects is concerned with inhomogeneous (trapped) atomic BEC's, it proves useful to mention a few properties of the homogeneous (uniform) Bose gas theory, since the two systems will share many features, at least qualitatively, when the density of the inhomogeneous gas is slowly varying. The low-density expansion of a homogeneous Bose gas of hard spheres of mass m is well known [11–13]. The expansion relies on an improved, though still shape-independent, potential over the pseudopotential of Eq. (1), called the regularized Fermi pseudopotential:

$$V_{\text{reg-pseudo}}(\mathbf{r}) = \frac{4\pi\hbar^2 a}{m}\delta(\mathbf{r})\frac{\partial}{\partial r}r. \tag{2}$$

The ground-state energy per particle, expanded in terms of the gas parameter $\sqrt{na^3}$, is

*Email address: dwatson@ou.edu

$$\frac{E}{N}=\frac{2\pi\hbar^2 na}{m}\left[1+\frac{128}{15\sqrt{\pi}}(na^3)^{1/2}+\frac{8(4\pi-3\sqrt{3})}{3}(na^3)\ln(na^3)+O(na^3)\right], \tag{3}$$

where n is the uniform number density. In this approximation, it is assumed that the gas is dilute, that is, the average interatomic spacing is much larger than the s-wave scattering length, stated mathematically as $na^3 \ll 1$. For larger densities, higher-order terms in the expansion beyond those in Eq. (3) are needed, and these terms depend on the detailed shape of the potential [14]. The leading-order term of Eq. (3) was first derived by Bogoliubov [11] and is equivalent to the mean-field term in the Gross-Pitavskii equation (see below). The term in Eq. (3) of order $(na^3)^{3/2}$ was derived by Lee, Huang, and Yang [12], and the logarithmic term was first obtained by Wu [13]. Lieb and Yngvason [15] showed that for a repulsive, non-negative, finite range, spherical, two-body potential, the Bogoliuobov mean-field term $E/N=2\pi\hbar^2 na/m$ is the *lower* bound for the exact ground-state energy of a homogeneous Bose gas. Giorgini *et al.* [7] found that Eq. (3) continues to be a good approximation for higher densities provided the logarithmic term is dropped. At intermediate densities ($na^3 > 1.385\times 10^{-3}$) the logarithmic term causes the overall correction [second and third terms in brackets in Eq. (3)] to the Bogoliuobov mean-field energy to become negative, thus, violating the lower bound. For a narrow range of na^3 the logarithmic term does actually improve the energy over the mean-field term.

The validity condition for a homogeneous gas to be described by the shape-independent approximation of Eq. (3) is given by the diluteness condition $na^3 \ll 1$. This condition is often invoked for the inhomogeneous system as well, except, since the density is not uniform, one uses some other characteristic density of the gas, usually the peak density at the center of the trap $n(0)$ [8,10,16]. However, it is possible for the condensate to be in a strongly interacting regime where the shape-independent approximation fails, and to still be dilute (i.e., $na^3 \ll 1$). In this paper, we use DPT to study both weakly and strongly interacting systems. In the latter case, we examine systems with both large atom number and large scattering length.

We consider three scattering lengths for a system of N trapped atoms: the natural ^{87}Rb scattering length, and multiples 10 and 100 times ^{87}Rb's value. Condensates at this largest value of the scattering length have been created in the lab [3]. As mentioned earlier, the shape-independent approximation is one of the underlying weaknesses of the GP equation. In this paper, "a proof-of-concept" study, we use a potential with a simple shape, namely, that of a hard sphere, for the interatomic interactions. This is a potential of choice for many-body theoretical studies since it is purely repulsive and has an s-wave scattering length equal to its radius. In a previous paper, we introduced the methods of many-body DPT for a general system of identical, interacting particles under spherically symmetric quantum confinement [17]. In the present study, we use this many-body formalism to calculate the ground-state energy for spherical condensates in both the strongly and weakly interacting regimes.

We compare our many-body results with two nonlinear field equations that describe inhomogeneous condensates: the mean-field Gross-Pitaevskii equation and a modified GP equation that contains beyond-mean-field quantum corrections. The GP energy for an isotropically trapped BEC is calculated from the following energy functional:

$$E_{GP}[\psi]=\int d\mathbf{r}\left[\frac{\hbar^2}{2m}|\nabla\psi|^2+\frac{1}{2}m\omega_{ho}^2 r^2|\psi|^2+\frac{2\pi\hbar^2(N-1)a}{m}|\psi|^4\right], \tag{4}$$

where ω_{ho} is the harmonic frequency of the isotropic trap and ψ is the ground-state field, which is given by the solution of the GP equation:

$$\left(-\frac{\hbar^2}{2m}\nabla^2+\frac{1}{2}m\omega_{ho}^2 r^2+\frac{4\pi\hbar^2(N-1)a}{m}|\psi|^2\right)\psi=\mu\psi. \tag{5}$$

In Eq. (5), μ is interpreted as the chemical potential in the Bogoliubov approach and as the ground-state orbital energy in the Hartree-Fock approach [18]. The presence of the quantity $(N-1)$ in the nonlinear term, rather than N, follows from number-conserving Schrödinger quantum mechanics with a product of orbitals as the initial state [18].

The so-called modified GP (MGP) equation includes an analytical quantum correction to the mean-field contribution from the GP equation [4,5]. This correction takes the form of an additional nonlinear term to the GP energy functional, which arises from the ground-state depletion of the condensate due to excitations. The MGP energy is calculated from the following energy functional:

$$E_{MGP}[\psi]=\int d\mathbf{r}\left[\frac{\hbar^2}{2m}|\nabla\psi|^2+\frac{1}{2}m\omega_{ho}^2 r^2|\psi|^2+\frac{2\pi\hbar^2(N-1)a}{m}|\psi|^4\left(1+\frac{128}{15\sqrt{\pi}}a^{3/2}(N-1)^{1/2}\psi\right)\right], \tag{6}$$

where the field is given by the following nonlinear Schrödinger equation:

$$\left[-\frac{\hbar^2}{2m}\nabla^2+\frac{1}{2}m\omega_{ho}^2 r^2+\frac{4\pi\hbar^2(N-1)a}{m}|\psi|^2\times\left(1+\frac{32}{3\sqrt{\pi}}a^{3/2}(N-1)^{1/2}\psi\right)\right]\psi=\mu\psi. \tag{7}$$

The MGP energy was derived by Braaten and Nieto [4] by carrying out a self-consistent one-loop calculation through second order in the gradient expansion. In Eqs. (6) and (7) we have dropped the additional nonlocal term in Eq. (2) of Ref. [4] that accounts for edge effects since it is found to be small [4,8]. The stationary MGP solution of Eq. (7) minimizes the MPG energy functional, Eq. (6). Although it includes some effects due to correlation, the MGP equation

like the GP equation, is still independent of the shape of the interatomic potential.

The nonlinear term in the GP energy functional, Eq. (4), reproduces the leading-order term of the homogeneous energy density expansion, Eq. (3), in the uniform limit. Likewise, the nonlinear terms in the MGP energy functional, Eq. (6), reproduce the homogeneous-gas energy per particle of Eq. (3) with the logarithmic term neglected (see Appendix A). Equation (6) is the inhomogeneous generalization of the first two terms in Eq. (3).

We compare our results with the GP and MGP equations (5) and (7), respectively, and discuss the relevance of the logarithmic term in Eq. (3) to the range of validity of our DPT results. In addition to predicting ground-state properties of the condensate, we also calculate excitation properties, such as frequencies, which arise naturally from our first-order calculation. Excitations involving compression such as the breathing mode will emphasize the breakdown of the shape-independent mean-field approximation. An advantage of many-body DPT over purely numerical methods is the analytical nature of its results which offer insight into the many-body physics of BEC.

In Sec. II we discuss the formalism of many-body DPT and give analytical expressions for the ground-state energy and normal-mode frequencies. We also introduce our dimensionally continued parametrization of the hard-sphere potential and in Sec. IV we describe how the many-body interaction parameters are optimized to give the best energies. Results and interpretation of the ground state are given in Sec. V where we discuss the range of validity of our results in terms of the low-density expansion, Eq. (3). In Sec. VI we give beyond-mean-field breathing mode frequencies and in Sec. VII we summarize and discuss how to improve and extend our results.

II. FORMALISM

A. The dimensionally scaled Schrödinger equation

The N-body Schrödinger equation for a system of identical, trapped, interacting particles in D-dimensional Cartesian coordinates is

$$H\Psi = \left[\sum_{i=1}^{N} h_i + \sum_{i=1}^{N-1} \sum_{j=i+1}^{N} g_{ij} \right] \Psi = E\Psi , \tag{8}$$

$$h_i = -\frac{\hbar^2}{2m} \sum_{\nu=1}^{D} \frac{\partial^2}{\partial x_{i\nu}^2} + V_{\mathrm{conf}} \left(\left[\sum_{\nu=1}^{D} x_{i\nu}^2 \right]^{1/2} \right), \tag{9}$$

$$g_{ij} = V_{\mathrm{int}} \left(\left[\sum_{\nu=1}^{D} (x_{i\nu} - x_{j\nu})^2 \right]^{1/2} \right), \tag{10}$$

where V_{conf} is the trapping potential, V_{int} is the two-body interatomic potential, H is the D-dimensional Hamiltonian, and $x_{i\nu}$ is the νth Cartesian component of the ith particle. We have also assumed equal masses m for the condensate atoms at $T=0$ K, which are confined by an isotropic, harmonic trap with frequency ω_{ho}:

$$V_{\mathrm{conf}}(r_i) = \tfrac{1}{2} m \omega_{ho}^2 r_i^2 . \tag{11}$$

We take the interatomic potential to be a hard sphere of radius a:

$$V_{\mathrm{int}}(r_{ij}) = \begin{cases} \infty, & r_{ij} < a \\ 0, & r_{ij} \geqslant a , \end{cases} \tag{12}$$

where a is the s-wave scattering length of the condensate atoms. We dimensionally continue the hard-sphere potential so that it is differentiable away from $D=3$, allowing us to perform the dimensional perturbation analysis (see Ref. [17] as well as a later discussion in this paper). Thus, we take the interaction to be

$$V_{\mathrm{int}}(r_{ij}) = \frac{V_o}{1-3/D} \left\{ 1 - \tanh \left[\frac{c_o}{1-3/D} \left(r_{ij} - \alpha - \frac{3}{D}(a-\alpha) \right) \times \left(1 + (1-3/D) \sum_{n=1}^{s-3} c_n r_{ij}^{2n} \right) \right] \right\}, \tag{13}$$

where D is the Cartesian dimensionality of space. This interaction becomes a hard sphere of radius a in the physical, $D=3$, limit. The other s constants (V_o, α, and $\{c_n ; \forall n : 0 \leqslant n \leqslant s-3\}$) are parameters that allow us to fine-tune the large-D shape of the potential and optimize our results through Langmuir (first) order (see Sec. IV). The simplest possibility could have as few as two parameters V_o and c_o, with $\alpha = a$ and the remaining $c_n = 0$; however, we can have any number of parameters for the most general and flexible potential. The form of the potential at $D \neq 3$ is not unique. Other forms could be chosen with equal success as long as the form is differentiable and reduces to a hard-sphere potential at $D=3$. We simply choose a form that allows a gradual softening of the hard wall.

In this paper, we restrict our attention to spherically symmetric states (i.e., s-wave states), and we now transform the Schrödinger equation to a form more suitable for dimensional perturbation-theory analysis. The transformation, discussed fully in Ref. [17], takes place in three steps. The first step is to transform the variables of all N particles, each with D Cartesian components $x_i = (x_{i1}, x_{i2}, \ldots, x_{iD})$ $(1 \leqslant i \leqslant N)$, to internal coordinates, defined as the D-dimensional scalar radii r_i of the N particles and the angle cosines γ_{ij} of the $N(N-1)/2$ angles between the radial vectors:

$$r_i = \sqrt{\sum_{\nu=1}^{D} x_{i\nu}^2} \quad (1 \leqslant i \leqslant N) \quad \text{and} \tag{14}$$

$$\gamma_{ij} = \cos(\theta_{ij}) = \left(\sum_{\nu=1}^{D} x_{i\nu} x_{j\nu} \right) \Big/ \, r_i r_j \quad (1 \leqslant i < j \leqslant N).$$

The second step is to carry out a similarity transformation of the Schrödinger equation resulting from the first step. The transforming function

$$\chi = (r_1 r_2 \cdots r_N)^{-(D-1)/2} \Gamma^{-(D-1)/4} \tag{15}$$

results in a Schrödinger equation in terms of $\Phi(=\chi^{-1}\Psi)$, in which the first derivative terms of the Laplacian are removed.

The third step is to regularize the large-D limit of the similarity-transformed Hamiltonian ($\chi^{-1}H\chi$). We do this by converting the variables to dimensionally scaled harmonic-oscillator units (bars):

$$\overline{r_i} = \frac{r_i}{D^2 \overline{a_{ho}}}, \quad \overline{E} = \frac{D^2}{\hbar \overline{\omega_{ho}}} E, \quad \overline{H} = \frac{D^2}{\hbar \overline{\omega_{ho}}} H, \quad \overline{a} = \frac{a}{\sqrt{2} D^2 \overline{a_{ho}}},$$

$$\overline{V_o} = \frac{D^2}{\hbar \overline{\omega_{ho}}} V_o, \quad \overline{\alpha} = \frac{\alpha}{\sqrt{2} D^2 \overline{a_{ho}}}, \quad \overline{c_o} = \sqrt{2} D^2 \overline{a_{ho}} c_o, \tag{16}$$

$$\overline{c_n} = (\sqrt{2} D^2 \overline{a_{ho}})^{2n} c_n,$$

where

$$\overline{a_{ho}} = \sqrt{\frac{\hbar}{m \overline{\omega_{ho}}}} \quad \text{and} \quad \overline{\omega_{ho}} = D^3 \omega_{ho} \tag{17}$$

are the dimensionally scaled harmonic-oscillator length and dimensionally scaled trap frequency, respectively. The dimensionally scaled harmonic-oscillator units of energy, length, and time are $\hbar\overline{\omega_{ho}}$, $\overline{a_{ho}}$, and $1/\overline{\omega_{ho}}$, respectively. All barred constants ($\overline{a}$, $\overline{a_{ho}}$, $\overline{\omega_{ho}}$, $\overline{V_o}$, $\overline{\alpha}$, $\overline{c_o}$, and $\overline{c_n}$) are held fixed as D varies. For example, as D varies $\overline{a}$ is held fixed at a value by requiring that it give the physical unscaled scattering length at $D=3$. Finally, we arrive at

$$\overline{H}\Phi = (\mathcal{T} + U + V)\Phi = \overline{E}\Phi, \tag{18}$$

where

$$\mathcal{T} = -\frac{1}{2}\delta^2 \sum_{i=1}^{N} \left[\frac{\partial^2}{\partial \overline{r_i^2}} + \sum_{j\neq i} \sum_{k\neq i} \frac{\gamma_{jk} - \gamma_{ij}\gamma_{ik}}{\overline{r_i^2}} \frac{\partial^2}{\partial \gamma_{ij} \partial \gamma_{ik}} \right], \tag{19}$$

$$U = \sum_{i=1}^{N} \frac{(\delta - 1)[(2N+1)\delta - 1]}{8\overline{r_i^2}} \frac{\Gamma^{(i)}}{\Gamma}, \tag{20}$$

$$V = \sum_{i=1}^{N} \frac{1}{2}\overline{r_i^2} + \frac{\overline{V_o}}{1-3\delta} \sum_{i=1}^{N} \sum_{j=i+1}^{N} \left\{ 1 - \tanh \left[\frac{\overline{c_o}}{1-3\delta} \left(\frac{\overline{r_{ij}}}{\sqrt{2}} - \overline{\alpha} - 3\delta(\overline{a} - \overline{\alpha}) \right) \left(1 + (1-3\delta) \sum_{n=1}^{s-3} \frac{\overline{c_n} \overline{r_{ij}}^{2n}}{2^n} \right) \right] \right\}, \tag{21}$$

where the perturbation parameter is

$$\delta = 1/D \tag{22}$$

and $\overline{r_{ij}} = \sqrt{\overline{r_i^2} + \overline{r_j^2} - 2\overline{r_i r_j}\gamma_{ij}}$ is the interatomic separation. The quantity $\mathcal{T}$ is the derivative portion of the kinetic energy $T = \mathcal{T} + U$. As D becomes infinitely large, and $\delta \to 0$, the entire differential part of the kinetic energy as well as a portion of the interatomic and centrifugal-like potentials will drop out of the Hamiltonian. In the infinite-dimension limit, the particles behave as though they become infinitely heavy and rest at the bottom of the infinite-D effective potential, a potential that includes the trap potential and contributions from the centrifugal-like and hard-sphere potentials. The infinite-D energy becomes the minimum value of the effective potential (see Appendix A of Ref. [19]).

As noted above, for a given set of trap parameters at $D=3$, the energy of the $D=3$ Bose-Einstein condensate depends only on the scattering length of the interatomic potential and not the detailed shape of the potential. This is due to the long-wavelength nature of BEC's: for small to moderate scattering lengths, the atomic wavelengths are not short enough to "resolve" the short-range detail of the potential. However, for large D the atomic wavelengths become very short, since according to Eqs. (18), (19), and (22) the scaled, similarity-transformed Hamiltonian displays an effective mass term equal to D^2. Thus, unlike at $D=3$, the energy of the large-D system is sensitive to the details of the potential.

One may think, *prima facie*, that this is an indication that the large-dimension limit is a poor starting point for a series expansion in terms of a perturbation parameter, in this case δ, since it appears not to reflect the long-wavelength nature of the condensate and displays a sensitivity to the details of the interatomic potential. These concerns are particularly acute since a large-order calculation for a large-N system seems infeasible. These concerns, though, are resolved upon closer inspection of the issues involved. Suppose one had actually found a perturbation scheme in some parameter which at low orders displays an insensitivity to the precise shape of the interatomic potential, as long as the perturbation parameter and scattering length are unchanged. Now what is most important in a low-order perturbation calculation is that the energy be as close as possible to the actual $D=3$ result. One could not, however, reasonably expect the energy at low orders to be both insensitive to the precise shape of the interatomic potential for fixed scattering length and, at the same time, to differ only a small amount from the actual $D=3$ condensate energy. The energy at low orders would almost certainly be different from the actual $D=3$ condensate.

In fact, instead of being a liability, this large-D sensitivity to the details of the interatomic potential is actually to our advantage, enabling us to optimize our dimensional continuation of the hard-sphere potential so that the low-order DPT energy is as close as possible to the actual $D=3$ result. We discuss this in detail in Sec. V.

Actually the issue of long wavelengths at $\delta = 1/3$ and short wavelengths for extremely small δ is a spurious concern. At $D=3$ the zeroth-order wave function does have a large-wavelength character, but further discussion of this issue is put off until Sec. II C.

B. Leading-order energy term

The infinite-D ($\delta \to 0$) effective potential in dimensionally scaled harmonic-oscillator units of Eqs. (16) and (17) is

$$V_{\rm eff}=\sum_{i=1}^{N}\left(\frac{1}{8\overline{r_i^2}}\frac{\Gamma^{(i)}}{\Gamma}+\frac{1}{2}\overline{r_i^2}\right)+\overline{V_o}\sum_{i=1}^{N}\sum_{j=i+1}^{N}\left\{1-\tanh\left[\overline{c_o}\left(\frac{\overline{r_{ij}}}{\sqrt{2}}-\overline{\alpha}\right)\left(1+\sum_{n=1}^{s-3}\frac{\overline{c_n r_{ij}^{2n}}}{2^n}\right)\right]\right\}. \quad (23)$$

One can see from the double-sum term in $V_{\rm eff}$ that the large-D interatomic potential has become a soft sphere of radius approximately $\overline{\alpha}$ and height $2\overline{V_o}$. The slope of the soft wall is determined by $\overline{c_o}$, while the remaining $(s-3)$ parameters act to further refine the shape of the interatomic potential. The development of DPT using the basic three-parameter potential ($s=3$) is discussed at length in Ref. [17].

The s parameters are chosen with the goal of optimizing the energy perturbation series through first order in δ. In Sec. V we optimize the potential by fitting the energies through first order to DMC energies [8] at low atom number ($N\leqslant 100$), and since in our DPT analysis the number of atoms N is a parameter, we can readily extrapolate to larger N without large amounts of calculation. Further discussion on the optimization procedure and the range of validity of the extrapolation to larger N will follow in Secs. IV and V, respectively.

In scaled units, the zeroth-order ($D\to\infty$) approximation to the energy becomes

$$\overline{E_\infty}=V_{\rm eff}(\overline{r_\infty},\gamma_\infty), \quad (24)$$

where $\overline{r_\infty}$ and γ_∞ are the radius and angle cosine at the minimum of $V_{\rm eff}$. Assuming a totally symmetric configuration

$$\overline{r_i}=\overline{r_\infty}\ (1\leqslant i\leqslant N)\quad\text{and}\quad \gamma_{ij}=\gamma_\infty\ (1\leqslant i<j\leqslant N), \quad (25)$$

we find that the large-D radii and energy per atom are

$$\overline{r_\infty}=\{2[1+(N-1)\gamma_\infty]\}^{-1/2}, \quad (26)$$

$$\frac{\overline{E_\infty^{(DPT)}}}{N}=\frac{1+(N-2)\gamma_\infty}{(1-\gamma_\infty)[1+(N-1)\gamma_\infty]}\frac{1}{8\overline{r_\infty^2}}+\frac{1}{2}\overline{r_\infty^2}+\frac{N-1}{2}\overline{V_o}[1-\tanh(\Theta)], \quad (27)$$

where for simplicity of presentation we have defined the following:

$$\Theta=\overline{c_o}(\overline{r_\infty}\sqrt{1-\gamma_\infty}-\overline{\alpha})\left(1+\sum_{n=1}^{s-3}\overline{c_n r_\infty^{2n}}(1-\gamma_\infty)^n\right). \quad (28)$$

The derivation of the above equations is an extension of the derivation of Eqs. (26)–(28) for the basic $s=3$ potential. This later case is discussed in detail in Ref. [17].

The above quantities $\overline{r_\infty}$, $\overline{E_\infty^{(DPT)}}/N$, and Θ are determined by the large-D direction cosine γ_∞ of the angle between the particle radius vectors when $D\to\infty$, which is given by the negative solution of smallest magnitude of

$$\overline{V_o}\,\overline{c_o}\Upsilon\,\mathrm{sech}^2\,\Theta+\frac{2\gamma_\infty[2+(N-2)\gamma_\infty]}{(1-\gamma_\infty)^{3/2}\sqrt{2[1+(N-1)\gamma_\infty]}}=0, \quad (29)$$

$$\text{with}\quad \Upsilon=\left[1+\sum_{n=1}^{s-3}[(2n+1)\overline{c_n r_\infty^{2n}}(1-\gamma_\infty)^n-2n\overline{\alpha c_n r_\infty^{2n-1}}(1-\gamma_\infty)^{n-1/2}]\right]. \quad (30)$$

C. Normal modes and first quantum energy correction

To obtain the $1/D$ quantum correction to the energy for large but finite values of D, we expand about the minimum of the $D\to\infty$ effective potential, Eq. (23), and use the FG matrix method [20] to obtain the normal-mode frequencies of the condensate. We first define a configuration vector consisting of all $N(N+1)/2$ internal coordinates

$$\overline{y}^T=(\overline{r_1},\overline{r_2},\ldots,\overline{r_N},\gamma_{12},\gamma_{13},\ldots,\gamma_{N-1,N}), \quad (31)$$

where T is the transpose operator. We make the following substitutions for all radii and angle cosines:

$$\overline{r_i}=\overline{r_\infty}+\delta^{1/2}\overline{r_i'}, \quad (32)$$

$$\gamma_{ij}=\gamma_\infty+\delta^{1/2}\gamma_{ij}', \quad (33)$$

where $\delta=1/D$ is the expansion parameter, and we define a displacement vector consisting of the internal displacement coordinates [primed in Eqs. (32) and (33)]

$$\overline{y'}^T=(\overline{r_1'},\overline{r_2'},\ldots,\overline{r_N'},\gamma_{12}',\gamma_{13}',\ldots,\gamma_{N-1,N}'). \quad (34)$$

The first-order term in the Hamiltonian (in $\delta=1/D$) becomes

$$\hat{H}_1=-\frac{1}{2}\sum_{\mu=1}^{P}\sum_{\nu=1}^{P}\partial_{\overline{y'}_\mu}[G_{\mu,\nu}]_\infty\partial_{\overline{y'}_\nu}+\frac{1}{2}\sum_{\mu=1}^{P}\sum_{\nu=1}^{P}\overline{y'}_\mu[F_{\mu,\nu}]_\infty\overline{y'}_\nu+v_o, \quad (35)$$

where

$$P\equiv N(N+1)/2 \quad (36)$$

is the number of internal coordinates. The elements of **G** are found by comparing with $\mathcal{T}$ of Eq. (19), and the elements of **F** are found by evaluating the Hessian matrix of the effective potential at the infinite-D symmetric minimum [17]:

$$[F_{\mu\nu}]_\infty=\left[\frac{\partial^2 V_{\rm eff}}{\partial\overline{y'}_\mu\,\partial\overline{y'}_\nu}\right]_\infty. \quad (37)$$

The quantity v_o is a constant first-order energy shift [see Eq. (60) below], and the subscripts μ and ν refer to the components of the displacement vector $\overline{y'}$, whose elements are the internal displacement coordinates defined in Eqs. (32)–(34).

To make the connection with internal coordinates more explicit we adopt the following subscripts to identify the elements of **F**, **G**, and the product **GF**, which we will need shortly: (i,j) refers to elements associated with (r_i,r_j); (i,jk)

refers to (r_i, γ_{jk}) and (ij,kl) refers to $(\gamma_{ij}, \gamma_{kl})$, etc. See Sec. 4.1 of Ref. [17] for more details on the indical structure of the **FG** matrices.

The first-order Hamiltonian $\hat{H}_1$ of Eq. (35) gives the first-order energy correction $\overline{E_0}$ and zeroth-order similarity-transformed wave function Φ_0 through the Schrödinger equation

$$\hat{H}_1 \Phi_0 = \overline{E_0} \Phi_0. \tag{38}$$

The Wilson FG method shows that under a linear transformation

$$\overline{q'} = \mathbf{T} \overline{y'}, \tag{39}$$

the large-D similarity-transformed Schrödinger equation of Eq. (38) takes on the separable form

$$\left[-\tfrac{1}{2} \partial_{\overline{q'}} \frac{T}{\overline{q'}} \partial_{\overline{q'}} + \tfrac{1}{2} \overline{q'}^T \mathbf{\Lambda} \overline{q'} + v_0 \right] \Phi_0 = \overline{E_0} \Phi_0, \tag{40}$$

where $\mathbf{\Lambda}$ is a positive-definite diagonal matrix (see Appendix A of Ref. [17] with the identification $\mathbf{T}=\mathbf{UA}$). Thus the large-dimension similarity-transformed Schrödinger equation is separable into one-dimensional harmonic-oscillator wave functions in each of the $N(N+1)/2$ normal modes $\overline{q'_p}$, where $1 \leqslant p \leqslant N(N+1)/2$. If $\overline{\omega_p}$ is the corresponding normal-mode frequency, then the wave function is a product of $N(N+1)/2$ harmonic-oscillator wave functions

$$\Phi_0(\overline{y'}) = \prod_{p=1}^{N(N+1)/2} h_{n_p}(\overline{\omega_p}^{1/2} \overline{q'_p}), \tag{41}$$

where $h_{n_p}(\overline{\omega_p}^{1/2} q'_p)$ is a one-dimensional harmonic-oscillator wave function of frequency $\overline{\omega_p}$, and n_p is the oscillator quantum number, $0 \leqslant n_p < \infty$, which counts the number of quanta in each normal mode.

Having obtained Eq. (41) we are now in a position to address the above noted concern (in Sec. II A) that low-order DPT might not contain the right physics for the macroscopic, long-wavelength $D=3$ condensate since DPT is a perturbation expansion based on solutions to the semiclassical short-wavelength problem in a large number of spatial dimensions. In the notation of Eqs. (31) and (34), Eqs. (32) and (33) can be written as

$$\overline{y^T} = \overline{y^T_\infty} + \delta^{1/2} \overline{y'}^T, \tag{42}$$

where

$$\overline{y^T_\infty} = \overline{y^T} \Big|_{\substack{\overline{r_i} = \overline{r_\infty} \\ \gamma_{jk} = \gamma_\infty}} \quad \forall\, 1 \leqslant i \leqslant N \quad \text{and} \quad 1 \leqslant j < k \leqslant N. \tag{43}$$

Inserting Eq. (42) into Eq. (39) one obtains

$$\overline{q^T} = \overline{q^T_\infty} + \delta^{1/2} \overline{q'}^T, \tag{44}$$

where

$$\overline{q_\infty} = \mathbf{T} \overline{y_\infty}. \tag{45}$$

Then using Eq. (44) in Eq. (41) one obtains

$$\Phi_0(\overline{y}) = \prod_{p=1}^{N(N+1)/2} h_{n_p}\left(\left\{ \frac{\overline{\omega_p}}{\delta} \right\}^{1/2} (\overline{q_p} - [\overline{q_\infty}]_p) \right). \tag{46}$$

Equation (46) represents oscillations about the Lewis structure configuration $\overline{q_\infty}$ with frequencies $\{\overline{\omega_p}/\delta\}$. When δ is small (large dimensions) the frequencies $\{\overline{\omega_p}/\delta/\delta\}$ are very large and so according to Eq. (46) the zeroth-order wave function is strongly localized about $\overline{q}=\overline{q_\infty}$ (i.e., it features short wavelengths). However as δ takes on increasing positive values, $\{\overline{\omega_p}/\delta/\delta\}$ becomes less and less large, and so the zeroth-order wave function becomes increasingly extensive. That is, the wavelengths of the zeroth-order wave function at $\delta=1/3$ have become macroscopic. Thus, the zeroth-order DPT wave function for the Bose-Einstein condensate at $D=3$ appropriately has a macroscopic, long-wavelength character.

The Wilson FG method shows that the normal-mode coordinates are the solutions of the eigenvalue equation

$$\mathbf{GF} \overline{q'_p} = \lambda_p \overline{q'_p}, \tag{47}$$

where the eigenvalues λ_p are the diagonal entries of the diagonal force-constant matrix $\mathbf{\Lambda}$ in Eq. (40). Thus the normal-mode frequencies are related to λ_p in Eq. (47) by

$$\lambda_p = \overline{\omega_p^2}. \tag{48}$$

Equation (47) leads to the secular equation

$$\det(\lambda_p \mathbf{I} - \mathbf{GF}) = 0 \tag{49}$$

for λ_p.

Equation (49) provides a general formula for calculating the normal-mode frequencies in terms of the elements of the product **GF**. In Ref. [17] we derive analytical expressions for the normal-mode frequencies in terms of the highly symmetric **GF** matrix elements. To simplify the analytical normal-mode frequencies given below, we define the scalar quantities a through ι:

$$a = (GF)_{i,i} = G_a F_a$$

$$b = (GF)_{i,j} = G_a F_b \quad (i < j),$$

$$c = (GF)_{ij,i} = G_g F_e + (N-2) G_h (F_e + F_f) \quad (i < j),$$

$$d = (GF)_{jk,i} = G_g F_f + 2 G_h [F_e + (N-3) F_f] \quad (i \neq j < k \neq i),$$

$$e = (GF)_{i,ij} = G_a F_e \quad (i < j),$$

$$f = (GF)_{i,jk} = G_a F_f \quad (i \neq j < k \neq i),$$

$$g = (GF)_{ij,ij} = G_g F_g + 2(N-2) G_h F_h \quad (i < j),$$

$$h = (GF)_{ij,jk} = G_g F_h + G_h F_g + (N-2) G_h F_h + (N-3) G_h F_\iota \quad (i < j < k),$$

$$\iota = (GF)_{ij,kl} = G_g F_\iota + 4G_h F_h + 2(N-4)G_h F_\iota \quad (i<j, k<l), \tag{50}$$

where the expressions in Eq. (50) for the **GF** matrix elements of the Schrödinger equation (18) in terms of the **F** and **G** matrix elements were derived in Ref. [17]. The nonzero **F** and **G** matrix elements are given in Appendix B.

Although there are $N(N+1)/2$ different normal modes, there are only five distinct normal-mode frequencies. The five distinct eigenfrequencies of **GF** belong to three different irreducible representations of the symmetric group S_N [17,21]. One distinct frequency is given by

$$\overline{\omega}_2 = \sqrt{g - 2h + \iota}, \tag{51}$$

and we designate the set of normal modes with this frequency by the label **2** [17,21]. This set of normal modes has a multiplicity $d_{\mathbf{2}} = N(N-3)/2$ [i.e., there are $N(N-3)/2$ normal modes with the same frequency $\overline{\omega}_2$). Two other frequencies are given by

$$\overline{\omega}_{1^\pm} = \sqrt{\eta_1 \pm (\eta_1^2 - \Delta_1)^{1/2}}, \tag{52}$$

where

$$\eta_1 = \tfrac{1}{2}[a - b + g + (N-4)h - (N-3)\iota], \tag{53}$$

$$\Delta_1 = -(N-2)(c-d)(e-f) + (a-b)[g + (N-4)h - (N-3)\iota]. \tag{54}$$

The two sets of normal modes with the frequencies $\overline{\omega}_{1^\pm}$ are a mixture of asymmetric stretching and bending motions, and we designate them by the labels $\mathbf{1}^-$ and $\mathbf{1}^+$ [17,21]. Their multiplicities are $d_{\mathbf{1}^-} = d_{\mathbf{1}^+} = N-1$. The last two frequencies are determined from the equations

$$\overline{\omega}_{0^\pm} = \sqrt{\eta_0 \pm (\eta_0^2 - \Delta_0)^{1/2}}, \tag{55}$$

where

$$\eta_0 = \frac{1}{2}\left[a - (N+1)b + g + 2(N-2)h - \frac{(N-2)(N-3)}{2}\iota\right], \tag{56}$$

$$\Delta_0 = [a - (N+1)b]\left[g + 2(N-2)h + \frac{(N-2)(N-3)}{2}\iota\right] - \frac{N-1}{2}[2c + (N-2)d][2e + (N-2)f]. \tag{57}$$

The two sets of normal modes with the frequencies $\overline{\omega}_{0^+}$ and $\overline{\omega}_{0^-}$ are a mixture of symmetric stretching and bending motions, and correspond to the breathing mode and center of mass of the condensate, respectively. Designating these two sets of normal modes by the labels $\mathbf{0}^-$ and $\mathbf{0}^+$, they have multiplicities $d_{\mathbf{0}^+} = d_{\mathbf{0}^-} = 1$ (i.e., they are singlets) [17,21].

To first order in δ the energy is

$$\overline{E}^{(DPT)} = \overline{E}_\infty + \delta\overline{E}_o + O(\delta^2) = V_{\mathrm{eff}}(\overline{r}_\infty, \gamma_\infty) + \delta\left(\sum_{\mu=\{\mathbf{0}^\pm,\mathbf{1}^\pm,\mathbf{2}\}}\sum_{\mathbf{n}_\mu=0}^{\infty}\left(\mathbf{n}_\mu + \frac{1}{2}\right)d_{\mu,\mathbf{n}_\mu}\overline{\omega}_\mu + v_o\right) + O(\delta^2), \tag{58}$$

where $\mathbf{n}_\mu$ are the vibrational quantum numbers of the normal modes of the same frequency $\overline{\omega}_\mu$ (as such, $\mathbf{n}_\mu$ counts the number of nodes in a given normal mode). The quantity $d_{\mu,\mathbf{n}_\mu}$ is the occupancy of the manifold of normal modes with vibrational quantum number $\mathbf{n}_\mu$ and normal-mode frequency $\overline{\omega}_\mu$, i.e., it is the number of normal modes with the same frequency $\overline{\omega}_\mu$ and the same number of quanta $\mathbf{n}_\mu$. The total occupancy of the normal modes with frequency $\overline{\omega}_\mu$ is equal to the multiplicity of the root λ_μ, i.e.,

$$d_\mu = \sum_{n_\mu=0}^{\infty} d_{\mu,\mathbf{n}_\mu}, \tag{59}$$

where d_μ is the multiplicity of the μth root. Because of the factors of δ in the centrifugal-like and hard-sphere potentials [U and V of Eq. (18)], there is also a constant shift v_o in the first-order term of Eq. (58) given by

$$v_o = -\frac{N(N+1)[1+(N-2)\gamma_\infty]}{4\overline{r}_\infty^2[1+(N-1)\gamma_\infty](1-\gamma_\infty)} + 3\overline{V}_o\frac{N(N-1)}{2} \times\left\{1 - \tanh\Theta + \overline{c}_o\left[(\overline{a}-\overline{\alpha})\left(\sum_{n=1}^{s-3}\overline{c}_n\overline{r}_\infty^{2n}(1-\gamma_\infty)\right) - (\overline{r}_\infty\sqrt{1-\gamma_\infty} - \overline{a})\right]\mathrm{sech}^2\Theta\right\}, \tag{60}$$

where Θ is given by Eq. (28).

Using the definitions of the dimensionally scaled harmonic-oscillator units in Eqs. (16) and (17), we can undo the scalings to write the through-first-order DPT energy of Eq. (58) in regular oscillator units ($\hbar\omega_{ho}$) as

$$E^{(DPT)} = DV_{\mathrm{eff}}(\overline{r}_\infty, \gamma_\infty) + \left[\sum_{\mu=\{\mathbf{0}^\pm,\mathbf{1}^\pm,\mathbf{2}\}}\sum_{\mathbf{n}_\mu=0}^{\infty}\left(\mathbf{n}_\mu + \frac{1}{2}\right)d_{\mu,\mathbf{n}_\mu}\overline{\omega}_\mu + v_o\right] + O(\delta). \tag{61}$$

Since the normal-mode frequencies $\overline{\omega}_\mu$ do not depend on D, Eq. (61) shows that their values are equal to the physical ($D=3$) excitation frequencies of the condensate. It is also noteworthy that in the noninteracting limit the DPT energy series truncates at first order and gives the exact isotropic D-dimensional N-particle harmonic-oscillator energy. At its minimum the effective potential in regular oscillator units ($\hbar\omega_{ho}$) in the noninteracting limit becomes $E_\infty = D\overline{E}_\infty = DV_{\mathrm{eff}}(\overline{r}_\infty = 1/\sqrt{2}, \gamma_\infty = 0) = DN/2$, the ideal-gas energy. In the infinite-D limit, $r_\infty = \sqrt{D/2}$ is the infinite-D radius in

TABLE I. Ground-state energies in units $\hbar\omega_{ho}$ for small scattering length and low N. Column 2 contains DMC energies from Ref. [8] (statistical uncertainty in parentheses). Column 3 contains our many-body DPT energies. Columns 4 and 5 contain the GP [Eq. (5)] and MGP energies [Eq. (7)], respectively. We use ^{87}Rb mass and let $a=100$ a.u. and $\omega_{ho}=2\pi\times 77.87$ Hz, which corresponds to $a=0.00433a_{ho}$, in oscillator units.

N	DMC	DPT	GP	MGP
3	4.51036(2)	4.51035	4.51032	4.51032
5	7.53443(4)	7.53441	7.53432	7.53434
10	15.1537(2)	15.1537	15.1534	15.1535
20	30.640(1)	30.6396	30.638	30.639
50	78.96(1)	78.964	78.953	78.962
100	165.07(5)	165.089	165.06	165.11

TABLE II. Ground-state energies in units $\hbar\omega_{ho}$ for large scattering length and low N. Column 2 contains DMC energies from Ref. [8] (statistical uncertainty in parentheses). Column 3 contains our many-body DPT energies. Columns 4 and 5 contain the GP [Eq. (5)] and MGP energies [Eq. (7)], respectively. We use ^{87}Rb mass and let $a=10\,000$ a.u. and $\omega_{ho}=2\pi\times 77.87$ Hz, which corresponds to $a=0.433a_{ho}$, in oscillator units.

N	DMC	DPT	GP	MGP
2	3.3831(7)	3.38319	3.3040	3.3950
3	5.553(3)	5.5519	5.329	5.611
5	10.577(2)	10.5771	9.901	10.772
10	26.22(8)	26.2151	23.61	26.84
20	66.9(4)	67.01538	57.9	68.5
50	239.2(3)	239.18	196.12	243.45

regular oscillator units, also the expectation value $\langle r^2\rangle$ for the ground-state D-dimensional spherical harmonic oscillator. In addition, the excitation frequencies become the N-atom harmonic-oscillator frequencies: $\overline{\omega}_\mu=2$ for all μ. As the interatomic interaction increases, the strength of the interaction is reflected in the deviation from the above noninteracting values of the infinite-D radius and direction cosine as well as the excitation frequencies of the leading-order energy correction.

III. MOTIVATION FOR LOW-ORDER METHOD

Recall that the dimensionally continued interatomic potential becomes a hard sphere at $D=3$ with radius equal to the scattering length, but takes on the shape of a soft-sphere for larger D. The reason for choosing this dimensional continuation of the hard sphere is to facilitate the DPT analysis, which requires a differentiable effective potential. The exact shape of the soft sphere for dimensions departing from $D=3$ is determined by s built-in parameters. In this paper we consider three scattering lengths: the ^{87}Rb scattering length $a_{\mathrm{Rb}}=0.004\,33a_{ho}$, and two larger multiples $a=10a_{\mathrm{Rb}}$ and $a=100a_{\mathrm{Rb}}$. For these three scattering lengths, we optimize the s interatomic potential parameters by fitting our ground-state analytical energy through first order [Eq. (58) with $d_{\mathbf{0}^\pm,0}=d_{\mathbf{0}^\pm}\equiv 1$, $d_{\mathbf{1}^\pm,0}=d_{\mathbf{1}^\pm}\equiv N-1$, and $d_{\mathbf{2},0}=d_{\mathbf{2}}\equiv N(N-3)/2$, with the rest of the $d_{\mu,\mathbf{n}_\mu}=0\,\forall\,\mathbf{n}_\mu\geqslant 1$ and $\mu=\mathbf{0}^\pm,\mathbf{1}^\pm,\mathbf{2}$] at the physical ($D=3$) dimension to accurate, low-N, hard-sphere, ground-state DMC energies [8].

The fitted interatomic parameters for each scattering length are given in Sec. V where we extrapolate our fitted energies to large values of N. Note that our extrapolating function is not an arbitrary fitting function to the data. Rather, it is based on the dynamical approximation to the real system that is intrinsic to DPT, which includes contributions from all components of the Hamiltonian, including the kinetic, trap, and interaction terms, as well as correlation effects beyond the mean-field approximation. Furthermore, this low-order approximation is well defined and, in principle, can be systematically refined by using higher-order DPT [19,22].

IV. OPTIMIZATION OF THE INTERATOMIC PARAMETERS

A χ-square statistic is used to optimize the parameters of the dimensionally continued interatomic potential. We fit it to six accurate low-N DMC energies [8] for each scattering length (see column 1 of Tables I–III) by minimizing the following quantity [23] with respect to the set of parameters $\{V_o,\alpha\}\cup\{c_n;\forall n:0\leqslant n\leqslant s-3\}$:

$$\chi^2=\sum_{i=1}^{6}\left(\frac{E_i^{(DMC)}-E^{(DPT)}(N_i;V_o,\alpha,\{c_n\})}{\sigma_i}\right)^2, \qquad (62)$$

where $E_i^{(DMC)}$ is the DMC energy and σ_i is the statistical uncertainty for a condensate with atom number N_i [24]. The quantity $E^{(DPT)}(N_i;V_o,\alpha,\{c_n\})$ is the DPT energy approximation through first order given by Eq. (58) with interatomic potential parameters $\{V_o,\alpha\}\cup\{c_n;\forall n:0\leqslant n\leqslant s-3\}$. The Q probability is used to constrain the number of parameters s in the fitting function $E^{(DPT)}(N_i;V_o,\alpha,\{c_n\})$, where

TABLE III. Ground-state energies in units $\hbar\omega_{ho}$ for intermediate scattering length and low N. Column 2 contains DMC energies from Ref. [8] (statistical uncertainty in parentheses). Column 3 contains our many-body DPT energies. Columns 4 and 5 contain the GP [Eq. (5)] and MGP energies [Eq. (7)], respectively. We use ^{87}Rb mass and let $a=1\,000$ a.u. and $\omega_{ho}=2\pi\times 77.87$ Hz, which corresponds to $a=0.0433a_{ho}$, in oscillator units.

N	DMC	DPT	GP	MGP
3	4.6033(5)	4.6032	4.6007	4.6024
5	7.8356(15)	7.8356	7.8265	7.8340
10	16.426(6)	16.426	16.383	16.426
20	35.475(15)	35.474	35.297	35.497
50	103.99(3)	103.991	102.96	104.21
100	245.4(1)	245.402	241.85	246.24

$$Q\left(\frac{\nu}{2},\frac{\chi^2}{2}\right) \equiv \frac{\Gamma\left(\frac{\nu}{2},\frac{\chi^2}{2}\right)}{\Gamma\left(\frac{\nu}{2}\right)} \equiv \frac{1}{\Gamma\left(\frac{\nu}{2}\right)}\int_{\chi^2/2}^{\infty} e^{-t}t^{\nu/2-1}dt \quad (63)$$

is the probability that χ^2 should exceed a particular value by chance, and in our case [25] the quantity $\nu=6-s$ is the number of degrees of freedom in the fitting function [26]. We want to use the minimum number of parameters that extracts all of the relevant physical information from the DMC energies, and yet does not overfit the DMC energies. Thus, the number of parameters, s, is constrained to be the minimum number of parameters whose χ^2 gives a Q probability greater than 0.5. The value of $Q=0.5$ is chosen as the cutoff in order to avoid overfitting the DMC energies. Overfitting is a serious concern as we are extrapolating our energies to large N, and we wish to capture the essential information without fitting it to statistical fluctuations in the DMC energies. We found $s=4$ to be the optimal number of parameters in the $E^{(DPT)}$ fitting function that gives a Q probability of at least 0.5 from the weighted least-squares fit to the six low-N ($N<100$) DMC energies for all three scattering lengths considered in this study [27].

V. GROUND-STATE ENERGY

In this section we report calculations for a spherical condensate with trap frequency $\omega_{ho}=2\pi\times 77.87$ Hz. We consider three scattering lengths: $a=100$ a.u. or $0.004\,33a_{ho}$ in oscillator units ($a_{ho}=\sqrt{\hbar/m\omega_{ho}}$) approximately equal to the natural ^{87}Rb value and multiples 10 and 100 times this value, i.e., $a=1000$ a.u. or $0.0433a_{ho}$ and $a=10\,000$ a.u. or $0.433a_{ho}$. The scattering length $a=0.433a_{ho}$ is especially relevant to experiments observing beyond-mean-field effects, because condensates with a scattering length of 10 000 a.u. have been achieved in nonspherical traps [3].

A. Small scattering length

For $a=0.004\,33a_{ho}$, we determine the $s=4$ interatomic potential parameters, in the dimensionally scaled harmonic-oscillator units defined in Eqs. (16) and (17), to be $V_o=0.0257$, $\alpha=-0.464$, $c_o=1.402$, and $c_1=0.109$, with $\chi^2=0.20$ and $Q=0.90$. Table I shows a low-N comparison of energies for $a=0.004\,33a_{ho}$. Column 2 contains accurate DMC energies for a hard-sphere potential calculated previously in Ref. [8], where the statistical uncertainty is given in parentheses. Column 3 contains our many-body DPT energies, while columns 4 and 5 contain GP and MGP energies, which are calculated by using the wave functions from Eqs. (5) and (7), respectively, in the corresponding energy functionals [1]. In Fig. 1, we plot the energy shift per atom due to the interatomic interactions (i.e., we subtract the ideal-gas energy $3N/2$, in units of $\hbar\omega_{ho}$) for the GP, MGP, and DPT extrapolation for larger N. There is very little difference between any of these interaction energies because, for such a small scattering length and moderate atom number, the condensate is very dilute and weakly interacting. Consistent with low-N DMC calculations by Blume and Greene [8], the many-body DPT energy is slightly above the MGP and GP energies for low and moderate N, with the MGP energy being slightly above the GP energy. Going to higher N (beyond that shown in the plot), near 10^4 atoms the DPT energy falls below the GP energy.

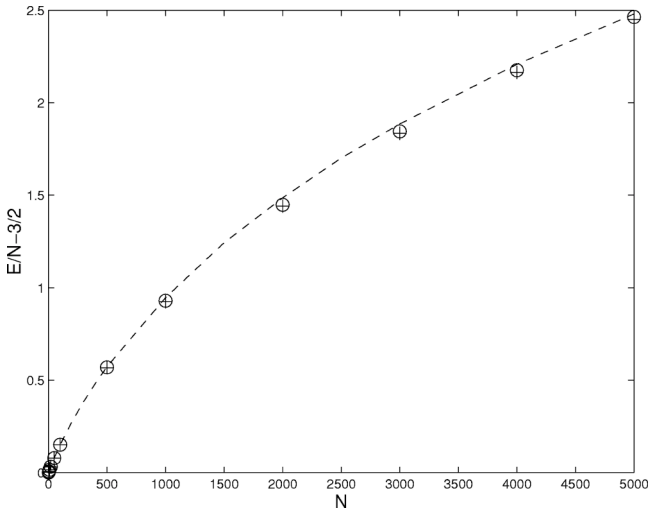

FIG. 1. Interatomic energy per atom vs number of condensate atoms for small scattering length. We use ^{87}Rb mass and let $a=100$ a.u. and $\omega_{ho}=2\pi\times 77.87$ Hz, which corresponds to $a=0.004\,33a_{ho}$, in oscillator units. Circles refer to the MGP energy from the solution of Eq. (7), plus signs, slightly below the circles, refer to the GP energy from the solution of Eq. (5), and the dashed line refers to the many-body DPT energy. Interaction energies are obtained by subtracting the ideal-gas energy $3N/2$ from the total energy. Energies are given in oscillator units ($\hbar\omega_{ho}$).

B. Large and intermediate scattering length

The $s=4$ interatomic potential parameters for the large scattering length $a=0.433a_{ho}$ are found to be $V_o=4.617\times 10^7$, $\alpha=-4.211$, $c_o=1.555$, and $c_1=5.00\times 10^{-3}$, with $\chi^2=0.23$ and $Q=0.89$. In Table II and Fig. 2 for $a=0.433a_{ho}$, it can again be seen that the MGP interaction energy lies above GP, but the DPT interaction energy is now sandwiched between MGP and GP. These results are also consistent with accurate low-N DMC calculations in Ref. [8], which show MGP overestimating the ground-state energy for $a=0.433a_{ho}$ for small N. However, as one increases the number of atoms beyond that displayed in Fig. 2, one finds that the low-order many-body DPT interaction energy eventually falls below GP above 10^4 atoms.

The intermediate-a ($a=0.0433a_{ho}$) interaction parameters are found to be $V_o=0.645$, $\alpha=-0.837$, $c_o=1.3875$, and $c_1=0.0889$, where $\chi^2=0.0047$ and $Q=0.998$. Figure 3 shows the DPT interatomic energy falling below GP at a few hundred atoms, as opposed to approximately 10^4 atoms for large and small a.

C. Discussion

The validity of our extrapolated DPT approach is demonstrated by the results for small a. For such a small scattering

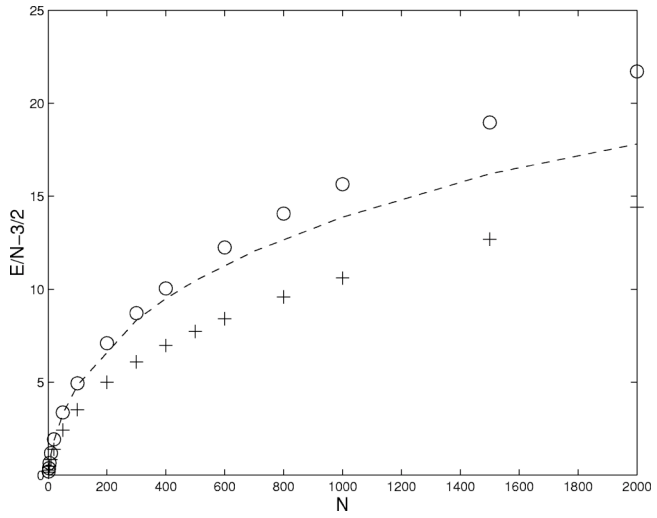

FIG. 2. Interatomic energy per atom vs number of condensate atoms for large scattering length. We use ^{87}Rb mass and let $a=10\,000$ a.u. and $\omega_{ho}=2\pi\times 77.87$ Hz, which corresponds to $a=0.433a_{ho}$, in oscillator units. Circles refer to the MGP energy from the solution of Eq. (7), plus signs refer to the GP energy from the solution of Eq. (5), and the dashed line refers to the many-body DPT energy. Interaction energies are obtained by subtracting the ideal-gas energy $3N/2$ from the total energy. Energies are given in oscillator units ($\hbar\omega_{ho}$).

length the mean-field GP energy is expected to be very close to the exact energy since we are in a dilute gas regime where many-body effects should be minimal. Indeed we see in Fig. 1 that there is little difference between the mean field and DPT energies for $a=0.004\,33a_{ho}$ validating our approach.

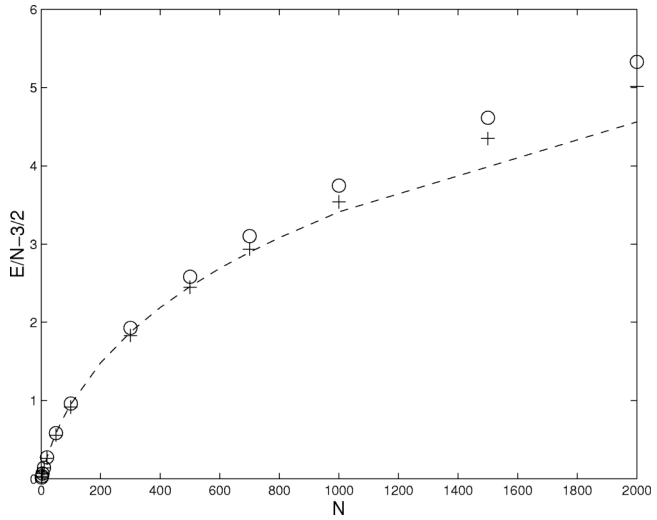

FIG. 3. Interatomic energy per atom vs number of condensate atoms for intermediate scattering length. We use ^{87}Rb mass and let $a=1\,000$ a.u. and $\omega_{ho}=2\pi\times 77.87$ Hz, which corresponds to $a=0.0433a_{ho}$, in oscillator units. Circles refer to the MGP energy from the solution of Eq. (7), plus signs refer to the GP energy from the solution of Eq. (5), and the dashed line refers to the many-body DPT energy. Interaction energies are obtained by subtracting the ideal-gas energy $3N/2$ from the total energy. Energies are given in oscillator units ($\hbar\omega_{ho}$).

The low-N DMC energies are a shade higher than the mean-field result and our extrapolated DPT energies remain a little higher than the mean-field result of $N=10\,000$ atoms. We attribute this to the inclusion in the DPT approach of correlation effects beyond mean field, and in this regard, as noted in the Introduction, the exact, fully correlated result for the homogeneous unconfined system also lies above the mean-field result [15]. However, we take the fact that the DPT result drops below the mean-field result beyond $N=10\,000$ to be an indication that the first-order DPT extrapolation has been extended beyond its range of validity. Presumably higher orders in the DPT expansion are needed beyond $N=10\,000$.

For large scattering lengths such as $a=0.433a_{ho}$, the condensate has entered a density regime where the mean-field approximation is no longer accurate and from Fig. 2 the GP approximation is clearly seen to fail. The DPT extrapolation agrees with the MGP approximation out to a few hundred atoms. As N increases, the DPT result drops below the shape-independent MGP result, and the difference gets larger as N becomes larger. The MGP energy functional, Eq. (6), is expected to yield energies that are too high as N becomes larger since, as discussed following Eq. (7), it is the *inhomogeneous* analog of the first two terms of the *homogeneous* gas expansion and neglects the logarithmic term which is negative in this regime. In fact, a simple estimate shows that the correction to the mean-field in Eq. (3), the sum of the last two terms, is already negative for $a=0.433a_{ho}$ for only a single atom [28]. This would seem to indicate that higher-order terms which are shape dependent are needed in the local-density approximation corresponding to Eq. (3). That is, the energies depend on the detailed shape of the potential, in this case the hard-sphere potential. Although the accurate DMC result indicates that the shape-independent mean field differs by only 2% from the accurate hard-sphere result at $N=50$ (see Table II), our DPT extrapolation (see Fig. 2) indicates that this difference, and also the difference from the MGP result, grows and becomes quite large by $N=2000$.

The DPT result drops below the mean-field result beyond $N=10\,000$ and, as for the small scattering length situation, this is an indication that the Langmuir-order DPT extrapolation has been extended beyond its range of validity and that higher orders in the DPT expansion are needed at very large N.

At intermediate a (i.e., $a=0.0433a_{ho}$) the DPT energies are likewise sandwiched between the GP and MGP results. Nonetheless, while the DPT energy for large and small a does not fall below GP energy until around $N=10^4$ atoms, Fig. 3 shows that for intermediate-a the DPT result falls below the GP result at a few hundred atoms. For this intermediate a, the interaction parameters are determined from exact DMC energies, but in a nearly shape-*independent* density regime [i.e., $n_{TF}(0)a^3<10^{-4}$], and then extrapolated into a shape-dependent regime [i.e., $n_{TF}(0)a^3>10^{-3}$]. The extrapolated energies appear qualitatively to follow the three-term local-density approximation of Eq. (3), which includes the logarithmic term but not higher-order, shape-dependent corrections, and falls below the mean-field first term for large enough na^3. This is to be expected since the intermediate-a potential parameters were calculated in a nearly shape-

independent density regime and so the low-order DPT terms do not uniquely relate to the hard-sphere potential. Other potentials, with the same $D=3$ scattering length, when dimensionally continued away from $D=3$ will have the same Lewis and Langmuir terms as the hard-sphere potential when fitted to similarly accurate low-N shape-independent DMC data. Thus the intermediate-a DPT extrapolation seen in Fig. 3 follows the shape-independent terms in the expansion of Eq. (3) with the DPT energy falling below the GP result at a few hundred atoms. To accurately extrapolate the DPT energy into the shape-dependent regime at intermediate a will require us to include the next term in the series which will manifest shape dependence. It should be noted that the reduced extrapolation range for intermediate a is not due to overfitting, the large Q-probability for four-parameters notwithstanding. The dramatic increase in Q from $s=3$ to $s=4$ parameters indicates underfitting for any $s<4$. Moreover, varying the fourth parameter above and below the optimal fit to lower the Q probability to 0.5 produces results with the same limited range of validity noted above.

The situation, though, is different for the small a and large a DPT results through Langmuir order where they have a significantly larger range of validity. We note that the fitted large-a (e.g., $a=0.433a_{ho}$) DPT potential parameters contain shape-dependent information since they are determined in a shape-dependent density regime. On the other hand, such as for the intermediate-a extrapolation, the low-a (e.g., $a=0.004\,33a_{ho}$) potential parameters were also determined in a shape-independent regime, but the extrapolated energies have yet to reach the shape-dependent regime. The local-density approximation of Eq. (3) and Ref. [28] suggests that the condensate does not enter the small-a shape-dependent regime until there are more than 10^9 atoms. The fact that the DPT energy falls below the GP energy at around $N=10^4$ atoms rather than 10^9 atoms indicates that higher-order terms are needed in the DPT expansion to obtain an accurate energy at low a before the shape-dependent regime is reached.

VI. EXCITATIONS

As we have noted in the Introduction, the additional compression found in excitations will accentuate the breakdown of the mean-field approximation. We can easily calculate excitation properties of the condensate, such as frequencies, from the normal-mode structure of many-body DPT. The analytical frequencies in Eq. (55), $\overline{\omega}_{0^-}$ and $\overline{\omega}_{0^+}$, correspond to the center of mass and breathing modes of the condensate, respectively. In units of the trap frequency ω_{ho}, the center-of-mass frequency equals 2. We also calculate the frequencies of small oscillation about the ground-state wave function within the mean-field approximation by solving the linearized GP equation [1].

Using the hydrodynamic theory of superfluids [29] based on the GP equation, Stringari found the following large-N approximation to the mean-field dispersion relation [30]:

$$\omega(n_r,l)=\omega_{ho}(2n_r^2+2n_rl+3n_r+l)^{1/2}, \tag{64}$$

where n_r is the number of radial nodes and l is the angular momentum of the excitation. Despite the significant departure from the noninteracting case $[\omega=\omega_{ho}(2n_r+l)]$, the mean-field frequency does not depend on the scattering length or the number of atoms in the Thomas-Fermi limit. This curious lack of dependence on the mean-field interaction strength Na/a_{ho} in the strongly interacting limit can be seen as a consequence of the relationship between the spatial extent of the condensate and the speed of sound at the center of the condensate [1]. The excitation frequency in the phonon regime is given by $\omega\sim c(r=0;Na/a_{ho})/\lambda(Na/a_{ho})$, where the wavelength $\lambda(Na/a_{ho})$ associated with the excitation and the speed of sound at the center of the gas $c(r=0;Na/a_{ho})$ are both functions of Na/a_{ho}. In the phonon regime, the excitation wavelength for an inhomogeneous gas is on the order of the size of the gas, which increases with increasing Na/a_{ho}. As the mean-field interaction strength increases, the speed of sound increases in the same ratio as the increase in the wavelength of the phononlike excitation. This lack of dependence on the number of atoms and the scattering length clearly becomes a problem in the strongly interacting regime, as can be seen in Fig. 4. For intermediate scattering lengths and moderate number of atoms, the excitation frequency is accurately described by the hydrodynamic approximation of Eq. (64), which is independent of N. However, just like the TF approximation for the ground-state energy of the GP equation, Eq. (64) is a good approximation of the mean-field theory in the strongly interacting limit but the mean-field theory *itself* breaks down.

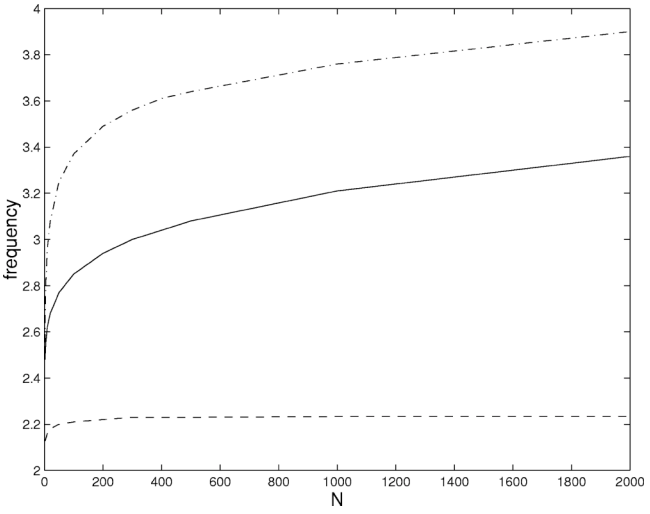

FIG. 4. Breathing mode frequency in units of ω_{ho} vs N for large scattering length. We use ^{87}Rb mass and let $a=10\,000$ a.u. and $\omega_{ho}=2\pi\times 77.87$ Hz, which corresponds to $a=0.433a_{ho}$, in oscillator units. The solid line corresponds to Eq. (65), the first correction to the monopole frequency calculated by Pitaevskii and Stringari [27]. The dashed line is the numerical solution of the linearized GP equation. The dash-dotted line refers to the DPT normal-mode frequency ω_{0^+} from Eq. (55).

In Ref. [31], Pitaevskii and Stringari consider beyond-mean-field corrections to the collective excitation frequencies in Eq. (64). Defining ω_M as the mean-field monopole frequency in the hydrodynamic limit [$n_r=1$, $l=0$ in Eq. (64)], ω as the hydrodynamic-limit beyond-mean-field frequency, and writing $\omega=\omega_M+\delta\omega_M$ (δ is not to be confused with $1/D$

as $\delta\omega_M$ is the shift from the mean-field monopole frequency), Stringari and Pitaevskii use the homogeneous gas first-order correction [i.e., the second term in Eq. (3)] to the Bogoliubov equation to find the following beyond-mean-field, but still shape-independent, fractional shift of the monopole (breathing mode) frequency in the hydrodynamic limit [27]:

$$\frac{\delta\omega_M}{\omega_M} = \frac{63}{256\sqrt{2}}[15N(a/a_{ho})^6]^{1/5}. \tag{65}$$

In Fig. 4 we compare the DPT breathing mode frequency ω_{0^+} in Eq. (55) with the mean-field (i.e., the solution of the linearized GP equation [1]) and the beyond-mean-field correction, Eq. (65), to the monopole (breathing) mode of frequency in the strongly interacting regime, $a=0.433a_{ho}$. The lack of dependence on the interaction strength for the mean-field excitation frequency in Eq. (64) is clearly a detriment in this regime, in which a large beyond-mean-field shift of the breathing mode frequency is predicted by both DPT and the beyond-mean-field calculation by Stringari and Pitaevksii. For $N=2000$ atoms we predict a fractional shift of 75% above the mean-field prediction while Eq. (65) gives a 50% shift.

VII. SUMMARY

Analytical and numerical results beyond the mean-field approximation have been obtained for the ground-state energy and breathing mode frequency of spherical atomic Bose-Einstein condensates with scattering lengths ranging from weakly to strongly interacting. We perform a low-order dimensional perturbation calculation in which N enters as a simple parameter in the energy expansion yielding results for all N from a single calculation. In this "proof-of-concept" paper we use a hard-sphere interaction, which we dimensionally continue so that it is differentiable in the infinite-D limit. This dimensional continuation results in a shape-dependent soft-sphere potential at large D and a hard sphere with radius equal to the scattering length in the physical $D=3$ limit. The large-D soft-sphere parameters are optimized for the ground-state energy.

We compare our semianalytical ground-state energy results with numerical solutions of the GP and modified GP equations for Bose-Einstein condensates with three different experimentally realizable scattering lengths [3], in the weakly, intermediately, and strongly interacting regimes. As expected, there is practically no deviation from the mean-field ground-state energy for small scattering length up to very large N validating our approach. For intermediate and large scattering lengths, though, the breakdown of the mean-field becomes quite noticeable even for a low number of atoms. At large scattering lengths our many-body DPT results seem to be accurate up to a fairly large atom number ($N\approx 10^4$). This is quite remarkable, given the complexity of the problem which involves approximately $N^2/2$ interactions. We also calculate collective excitation frequencies from our first-order normal-mode frequencies. In Eq. (55), the analytical frequency ω_{0^+} corresponds to the breathing mode of the condensate. The additional compression involved in excitations heightens the deviation from the mean-field result, and for the large scattering length, we predict a very large beyond-mean-field correction to the condensate breathing mode frequency. For $a=0.433a_{ho}$, for example, we predict a 75% fractional shift above the mean-field breathing mode frequency for $N=2000$ atoms.

For larger N, higher-order DPT terms, which are small for low and moderate N, will become significant and will need to be included in the calculation. Our studies suggest that the regime of validity through Langmuir order is more limited for intermediate scattering lengths since the transition from near shape independence to shape dependence occurs beyond the region of the reference data, but yet at moderate values of N. Incorporating higher-order terms in the perturbation series will extend the range of validity to larger N.

The results summarized above were obtained using a shape-dependent hard-sphere potential at $D=3$, a spherical trap, and perturbation terms through Langmuir order (first order). An obvious extension to this "proof-of-concept" study is the determination of higher-order terms in the perturbation series. As discussed in Sec. II C, the leading-order DPT wave function is a product of one-dimensional harmonic-oscillator wave functions with frequencies given by the first-order term of the energy series. From this wave function, one can then use ordinary perturbation theory to extend our results to include corrections beyond first order. For low N and low densities $[n(0)a^3 \leqslant 2\times 10^{-3}]$ our ground-state energies and excitation frequencies will depend only on the s-wave scattering length and not on any other details of the interatomic potential as demonstrated by Blume and Greene [8]. However as the condensate density becomes larger, the condensate energy and frequencies will become dependent upon the details of the particular potential. A comparison of results using other shape-dependent interatomic potentials such as a realistic Rb-Rb interatomic potential should provide further insight into this regime. In addition to including higher-order perturbation theory and testing other shape-dependent potentials, the generalization of the DPT formalism from spherical to cylindrical coordinates would enable a study of systems with axial symmetry, the predominant symmetry in current BEC experiments.

ACKNOWLEDGMENTS

This research was supported by the Office of Naval Research. We thank Doerte Blume for providing numerical DMC energies and for many helpful discussions.

APPENDIX A: HOMOGENEOUS LIMIT OF THE GP AND MGP EQUATIONS

Provided the density of the nonuniform gas is slowly varying, the uniform low-density expansion of Eq. (3) can be a useful tool for understanding the qualitative features of the inhomogeneous gas theory. We now show that one recovers the first two terms of the uniform Bose gas expansion of Eq. (3) from the GP and MGP energy functionals [Eqs. (4) and (6)] in the homogeneous limit. We first rewrite the GP energy

functional, Eq. (4), in terms of the ground-state density $n = N\psi^2$:

$$E_{GP}[n] = \int d\mathbf{r}\left[\frac{\hbar^2}{2m}|\boldsymbol{\nabla}\sqrt{n}|^2 + \frac{1}{2}m\omega_{ho}^2 r^2 n + \frac{2\pi\hbar^2 a}{m}n^2\right], \tag{A1}$$

where we have assumed a large number of atoms so that $N-1\approx N$. In the limit of a homogeneous gas in a box of volume V, the quantum pressure and the harmonic trap [the first and second terms in Eq. (A1)] become zero and the nodeless GP wave function becomes $\psi=\sqrt{1/V}$. The inhomogeneous energy functional, Eq. (A1), then reduces to the leading-order term of the homogeneous energy density expansion, Eq. (3), where $n=N/V$,

$$\frac{E_{GP}}{N} \to \frac{2\pi\hbar^2 na}{m}. \tag{A2}$$

In the homogeneous limit, the mean-field term of the GP equation is equivalent to the leading-order (Bogoliubov) term of the low-density expansion, Eq. (3).

Similarly, rewriting the MGP energy functional in terms of the ground-state density,

$$E_{MGP}[n] = \int d\mathbf{r}\left[\frac{\hbar^2}{2m}|\boldsymbol{\nabla}\sqrt{n}|^2 + \frac{1}{2}m\omega_{ho}^2 r^2 n + \frac{2\pi\hbar^2 a}{m}n^2 \times\left(1+\frac{128}{15\sqrt{\pi}}a^{3/2}\sqrt{n}\right)\right], \tag{A3}$$

and, as above, taking the homogeneous limit, one finds that the nonlinear terms in the MGP energy functional, Eq. (6), are equivalent to the energy per particle for a homogeneous gas in Eq. (3) with the logarithmic term neglected:

$$\frac{E_{MGP}}{N} \to \frac{2\pi\hbar^2 na}{m}\left[1+\frac{128}{15\sqrt{\pi}}(na^3)^{1/2}\right]. \tag{A4}$$

APPENDIX B: G AND F MATRICES

One of the advantages of dimensional perturbation theory is the simplifications that occur in the large-dimension limit, a limit in which one is able to find analytical expressions for the normal-mode frequencies of oscillation about the symmetric configuration. In particular, since we are dealing with identical particles in a totally symmetric configuration (the Lewis structure) in which all the particles are equivalent, the matrices **F**, **G**, and **GF**, collectively denoted by **Q**, display a high degree of symmetry with many identical elements. Specifically, their symmetry can be summarized by the following:

$$Q_{i,i} = Q_{i',i'} \equiv Q_a,$$

$$Q_{i,j} = Q_{i',j'} \equiv Q_b \quad (i\neq j) \quad \text{and} \quad (i'\neq j'),$$

$$Q_{ij,i} = Q_{i'j',i'} \equiv Q_c \quad (i\neq j) \quad \text{and} \quad (i'\neq j'),$$

$$Q_{jk,i} = Q_{j'k',i'} \equiv Q_d \quad (i\neq j\neq k) \quad \text{and} \quad (i'\neq j'\neq k'),$$

$$Q_{i,ij} = Q_{i',i'j'} \equiv Q_e \quad (i\neq j) \quad \text{and} \quad (i'\neq j'), \quad Q_{i,jk} = Q_{i',j'k'} \equiv Q_f \quad (i\neq j\neq k) \quad \text{and} \quad (i'\neq j'\neq k'),$$

$$Q_{ij,ij} = Q_{i'j',i'j'} \equiv Q_g \quad (i\neq j) \quad \text{and} \quad (i'\neq j'),$$

$$Q_{ij,jk} = Q_{i'j',j'k'} \equiv Q_h \quad (i\neq j\neq k) \quad \text{and} \quad (i'\neq j'\neq k'),$$

$$Q_{ij,kl} = Q_{i'j',k'l'} \equiv Q_\iota \quad (i\neq j\neq k\neq l) \quad \text{and} \quad (i'\neq j'\neq k'\neq l'). \tag{B1}$$

Note the indices in the relationships above run over all particles $(1,2,\ldots,N)$ with the exceptions noted in the far right column. For example, $Q_{i,j}=Q_{i',j'}\equiv Q_b$, where $(i\neq j)$ and $(i'\neq j')$, means that all off-diagonal elements of the pure radial quadrant of **Q** are equal to the same constant Q_b. Similarly, $Q_{ij,kl}=Q_{i'j',k'l'}\equiv Q_\iota$, where $(i\neq j\neq k\neq l)$ and $(i'\neq j'\neq k'\neq l')$ mean that any elements of **Q** in the pure angular quadrant that do not have a repeated index are all equal to the same constant Q_ι. We remark here that **G** and **F** are also symmetric matrices ($\mathbf{G}^T=\mathbf{G}$ and $\mathbf{F}^T=\mathbf{F}$); however, while the product **GF** does display the high degree of symmetry of Eq. (B1), it is not a symmetric matrix.

We now give the nonzero elements of the **G** and **F** matrices needed for the matrix product **GF** of Eq. (50). The **G** and **F** matrices are defined by the first-order $1/D$ Hamiltonian of Eq. (35). We can determine the elements of **G** by comparing the differential term in Eq. (35) with $\mathcal{T}$ of Eq. (19) expanded to first order in $1/D$. Using the notation in Eq. (B1), the nonzero elements of the **G** matrix are found to be

$$G_a = 1,$$

$$G_g = 2\frac{(1-\gamma_\infty^2)}{\bar{r}_\infty^2} = 4(1-\gamma_\infty)(1+\gamma_\infty)[1+(N-1)\gamma_\infty],$$

$$G_h = \frac{\gamma_\infty(1-\gamma_\infty)}{\bar{r}_\infty^2} = 2\gamma_\infty(1-\gamma_\infty)[1+(N-1)\gamma_\infty], \tag{B2}$$

where the matrix elements have been evaluated at the infinite-D symmetric minimum. Likewise, using Eq. (37), the nonzero **F** matrix elements are

$$F_a = 1+\frac{3}{4\bar{r}_\infty^4}\frac{1+(N-2)\gamma_\infty}{(1-\gamma_\infty)[1+(N-1)\gamma_\infty]} + \frac{\bar{V}_o\bar{c}_0}{2}(N-1) \times\operatorname{sech}^2\Theta\left[\bar{c}_o(1-\gamma_\infty)\Upsilon^2\tanh\Theta - \frac{1+\gamma_\infty}{2\bar{r}_\infty\sqrt{1-\gamma_\infty}}\right. + \sum_{n=1}^{s-3}\left(\frac{2n+1}{2}\bar{r}_\infty^{2n-1}(1-\gamma_\infty)^{n-1/2}[(2n-1)\gamma_\infty-(2n+1)]\right.$$

$$+ 2n\bar{\alpha}\bar{r}_\infty^{2n-2}(1-\gamma_\infty)^{n-1}[(n-1)\gamma_\infty - n]\Big)\bar{c}_n\Big],$$

$$F_b = \frac{\bar{V}_o\bar{c}_o}{2}\mathrm{sech}^2\,\Theta\Big[\bar{c}_o(1-\gamma_\infty)\Upsilon^2\tanh\,\Theta + \frac{1+\gamma_\infty}{2\bar{r}_\infty\sqrt{1-\gamma_\infty}} + \sum_{n=1}^{s-3}\Big(\frac{2n+1}{2}\bar{r}_\infty^{2n-1}(1-\gamma_\infty)^{n-1/2}[(2n+1)\gamma_\infty - (2n-1)] - 2n\bar{\alpha}\bar{r}_\infty^{2n-2}(1-\gamma_\infty)^{n-1}[n\gamma_\infty - (n-1)]\Big)\bar{c}_n\Big],$$

$$F_e = -\frac{\gamma_\infty}{2\bar{r}_\infty^3}\frac{1+(N-2)\gamma_\infty}{(1-\gamma_\infty)^2(1+(N-1)\gamma_\infty)^2} + \frac{\bar{V}_o\bar{c}_o}{2}\mathrm{sech}^2\,\Theta \times\Big[-\bar{c}_o\bar{r}_\infty\Upsilon^2\tanh\,\Theta + \frac{1}{2\sqrt{1-\gamma_\infty}} + \sum_{n=1}^{s-3}\frac{1}{2}\big((2n+1)^2 \times\bar{r}_\infty^{2n}(1-\gamma_\infty)^{n-1/2} - (2n)^2\bar{\alpha}\bar{r}_\infty^{2n-1}(1-\gamma_\infty)^{n-1}\big)\bar{c}_n\Big],$$

$$F_f = \frac{\gamma_\infty^2}{2\bar{r}_\infty^3(1-\gamma_\infty)^2[1+(N-1)\gamma_\infty]^2},$$

$$F_g = \frac{1}{2\bar{r}_\infty^2(1-\gamma_\infty)^3(1+(N-1)\gamma_\infty)^3}[1+3(N-2)\gamma_\infty + (13 - 12N + 3N^2)\gamma_\infty^2 + (N-2)(4-3N+N^2)\gamma_\infty^3] + \frac{\bar{V}_o\bar{c}_o}{2}\mathrm{sech}^2\,\Theta\Big[\frac{\bar{c}_o\bar{r}_\infty^2}{1-\gamma_\infty}\Upsilon^2\tanh\,\Theta + \frac{\bar{r}_\infty}{2(1-\gamma_\infty)^{3/2}} - \sum_{n=1}^{s-3}\Big(\frac{(2n-1)(2n+1)}{2}\bar{r}_\infty^{2n+1}(1-\gamma_\infty)^{n-3/2} - 2n(n-1)\bar{\alpha}\bar{r}_\infty^{2n}(1-\gamma_\infty)^{n-2}\Big)\bar{c}_n\Big],$$

$$F_h = \frac{-\gamma_\infty}{4\bar{r}_\infty^2(1-\gamma_\infty)^3(1+(N-1)\gamma_\infty)^3}[3+(5N-14)\gamma_\infty + (11-9N+2N^2)\gamma_\infty^2],$$

$$F_\iota = \frac{\gamma_\infty^2(2+(N-2)\gamma_\infty)}{\bar{r}_\infty^2(1-\gamma_\infty)^3(1+(N-1)\gamma_\infty)^3}. \tag{B3}$$

For more detail see Ref. [17].

[1] F. Dalfovo, S. Giorgini, L. P. Pitaevskii, and S. Stingari, Rev. Mod. Phys. **71**, 463 (1999).
[2] B. D. Esry and C. H. Greene, Phys. Rev. A **60**, 1451 (1999).
[3] S. L. Cornish, N. R. Claussen, J. L. Roberts, E. A. Cornell, and C. Wieman, Phys. Rev. Lett. **85**, 1795 (2000).
[4] E. Braaten and A. Nieto, Phys. Rev. B **56**, 14745 (1997).
[5] E. Timmermans, P. Tommasini, and K. Huang, Phys. Rev. A **55**, 3645 (1997).
[6] G. S. Nunes, J. Phys. B **32**, 4293 (1999).
[7] S. Giorgini, J. Boronat, and J. Casulleras, Phys. Rev. A **60**, 5129 (1999).
[8] D. Blume and C. H. Greene, Phys. Rev. A **63**, 063061 (2001).
[9] A. Fabrocini and A. Polls, Phys. Rev. A **60**, 2319 (1999).
[10] A. Fabrocini and A. Polls, Phys. Rev. A **64**, 063610 (1999).
[11] N. N. Bogoliubov, J. Phys. (Moscow) **11**, 23 (1947).
[12] T. D. Lee, K. Huang, and C. N. Yang, Phys. Rev. **106**, 1135 (1957).
[13] T. T. Wu, Phys. Rev. **115**, 1390 (1959).
[14] N. Hugenholtz and D. Pines, Phys. Rev. **116**, 489 (1959).
[15] E. H. Lieb and J. Yngvason, Phys. Rev. Lett. **80**, 2504 (1998).
[16] J. L. DuBois and H. R. Glyde, Phys. Rev. A **63**, 023602 (2001).
[17] B. A. McKinney, M. Dunn, D. K. Watson, and J. G. Loeser, Ann. Phys. (N.Y.) **310**, 56 (2004).
[18] B. D. Esry, Phys. Rev. A **55**, 1147 (1997).
[19] M. Dunn, T. Germann, D. Goodson, C. Traynor, J. Morgan III, D. Watson, and D. Herschbach, J. Chem. Phys. **101**, 5987 (1994).
[20] E. B. Wilson, J. C. Decius, and P. C. Cross, *Molecular Vibrations: The Theory of Infrared and Raman Vibrational Spectra* (McGraw-Hill, New York, 1955).
[21] J. G. Loeser, J. Chem. Phys. **86**, 5635 (1987).
[22] J. R. Walkup, M. Dunn, and D. K. Watson, Phys. Rev. A **63**, 025405 (2001).
[23] P. R. Bevington and D. K. Robinson, *Data Reduction and Error Analysis for the Physical Sciences* (McGraw-Hill, New York, 1992).
[24] The uncertainties in the DMC energies are a combination of statistical and systematic uncertainties. The systematic uncertainties are thought to be small [D. Blume (private communication)].
[25] Equation (62) assumes one can achive an exact fit $Q=1.0$ with $s=6$ parameters, which is not quite possible with our fitting function. However, the fit with $s=6$ parameters is close enough to effectively give $Q=1.0$
[26] W. H. Press, S. A. Teukolsky, W. T. Vetterling, and B. P. Flannery, *Numerical Recipes*, 2nd ed. (Cambridge University Press, Cambridge, 1992).
[27] In practice, there are three-parameter potential fits with Q values slightly over 0.5. The four-parameter extrapolations, however, are clearly superior to the three-parameter extrapolations. Since the errors on the DMC energies are the result of a conservative appraisal [D. Blume (private communication)], we take the four-parameter potential fits to be optimal and attribute the Q values being slightly over 0.5 for the three-parameter fits to the cautious error analysis.

[28] Strictly speaking, the truncated homogeneous gas expansion, Eq. (3), is only valid for low-density homogeneous hard-core Bose gases. However, if we assume the spatial variation of the inhomogeneous gas is not too abrupt, it seems reasonable to assume that the MGP functional for the inhomogeneous gas would result in energies that are also too high. We can use the expansion for the homogeneous gas, Eq. (3), to estimate the effect of the next correction to our MGP results as N varies. One can show that even for small atom numbers, at this large value of the scattering length, the gas parameter na^3 becomes large enough such that the logarithmic term becomes increasingly negative. If we use the TF peak density as the characteristic density we can approximate the gas parameter as $n_{TF}(0)a^3=[15N(a/a_{ho})^6]^{2/5}/8\pi$. The TF peak density is often a surprisingly good estimate of the Bose number density at the center of the trap, even when the TF energy is a poor approximation. DuBois and Glyde [16] show that for $Na/a_{ho}>5$ and $n(0)a^3<10^{-3}$, $n_{TF}(0)$ is a good estimate and it is sufficient for our qualitative use of Eq. (3). Using the above equation as the estimate for na^3, the correction to the mean field in Eq. (3), the sum of the last two terms, is already negative for $a=0.433\ a_{ho}$ for only a single atom.

[29] P. Nozières and D. Pines, *The Theory of Quantum Liquids* (Addison-Wesley, Reading, MA, 1990), Vol. II.

[30] S. Stringari, Phys. Rev. Lett. **77**, 2360 (1996).

[31] L. Pitaevskii and S. Stringari, Phys. Rev. Lett. **81**, 4541 (1998).